

Continuous Flow Total Artificial Heart: Modeling and Feedback Control in a Mock Circulatory System

HASSAN A. KHALIL,* DANIEL T. KERR,* MATTHEW A. FRANCKE,† RALPH W. METCALFE,† ROBERT J. BENKOWSKI,‡
WILLIAM E. COHN,*† EGEMEN TUZUN,* BRANISLAV RADOVANCEVIC,* O. H. FRAZIER,* AND KAMURAN A. KADIPASAOGLU*†

We developed a mock circulatory loop and used mathematical modeling to test the *in vitro* performance of a physiologic flow control system for a total artificial heart (TAH). The TAH was constructed from two continuous flow pumps. The objective of the control system was to maintain loop flow constant in response to changes in outflow resistance of either pump. Baseline outflow resistances of the right (pulmonary vascular resistance) and the left (systemic vascular resistance) pumps were set at 2 and 18 Wood units, respectively. The corresponding circuit flow was 4 L/min. The control system consisted of two digital integral controllers, each regulating the voltage, hence, the rotational speed of one of the pumps. The *in vitro* performance of the flow control system was validated by increasing systemic and pulmonary vascular resistances in the mock loop by 4 and 8 Wood units (simulating systemic and pulmonary hypertension conditions), respectively. For these simulated hypertensive states, the flow controllers regulated circuit flow back to 4 L/min within seconds by automatically adjusting the rotational speed of either or both pumps. We conclude that this multivariable feedback mechanism may constitute an adequate supplement to the inherent pressure sensitivity of rotary blood pumps for the automatic flow control and left-right flow balance of a dual continuous flow pump TAH system. *ASAIO Journal* 2008; 54: 249–255.

Successful long-term clinical use of continuous flow ventricular assist devices has stimulated investigation of their use as a total heart replacement. Because they are smaller than pulsatile pumps, continuous flow pumps (CFPs) are more easily used in children and smaller adults. Furthermore, CFPs have the potential for higher durability and lower power consumption, as well as lower cost than their pulsatile counterparts.^{1,2} Although, to date, the CFPs in clinical use as left ventricular assist devices have not been pumped to failure, it is noteworthy that the longest continuous application in one patient has exceeded 7 years. These favorable properties of CFPs have led us to conceive and develop a continuous flow total artificial heart (CFTAH), which consists of two CFPs replacing the ex-

cised ventricles, with the expectation to potentially broaden the clinical application of TAH technology and reduce the technical limitations of available TAH modalities.

A unique feature of CFPs is their ability to autoregulate flow output in response to varying inlet and outlet pressure conditions (see Appendix A). This intrinsic property makes CFPs particularly conducive to use in total heart replacement as, in tandem configuration, the output of one pump determines the inflow pressure (preload) of the other.^{3,4} The changes in right and left heart output, required to meet fluctuations in the physiologic demand, would thus occur simultaneously and instantaneously, as an automatic response to changes in systemic and pulmonary filling pressures. The regulated flow, in turn, would maintain the filling pressures in the vicinity of physiologic range. This intrinsic feedback mechanism that exists between the loading conditions and flow output of each pump individually, and between the respective outputs and inputs of both pumps in series, would conveniently minimize the need for external intervention for purposes of adjusting pump operation to meet patient physiology. CFTAH studies in the bovine and the ovine are currently ongoing in our laboratory, and continue to provide valuable information for validating the concept, refining the surgical technique, and optimizing the medical management.^{1,5}

Despite its sensitivity to preload and afterload, the autoregulatory potential of the CFTAH system described above may be challenged during extremes of cardiovascular physiologic conditions. Our preliminary experiments in mock circuits with tandem CFPs (without a pulse simulator to duplicate the native ventricles, which are excised in this clinical scenario⁶) have suggested that sudden changes in flow resistance (*i.e.*, vascular tone) and fluid pressure (*i.e.*, hypertension), or drainage of a significant fluid volume from the circuit (*i.e.*, hypovolemia), can induce prolonged periods of hemodynamic instability and/or atrial suction. As various control systems are already being investigated clinically for left ventricular assist devices to prevent inflow suction and regulate pump flow,^{7–11} we hypothesized that a feedback control system can maintain the cardiac output stable in the presence of such sudden and unanticipated hemodynamic fluctuations in our CFTAH.

We operated the above mock circulatory system to replicate the physiologic hemodynamics of the mammalian circulation. Using the pressure and flow data generated from the mock circulatory system, we derived a multiple-input/multiple-output mathematical model. On the basis of this mathematical model, we designed a physiologic-based CFTAH flow control system, which we evaluated within the same mock circulation. We report here the design of the mock circuit, the derivation of the

From the *Cardiovascular Surgical Research Laboratories, Texas Heart Institute at St. Luke's Episcopal Hospital; †Mechanical and Biomedical Engineering, University of Houston; and ‡MicroMed Cardiovascular, Houston, Texas.

Submitted for consideration August 2007; accepted for publication in revised form January 2008.

Reprint Requests: O. H. Frazier, M.D., Texas Heart Institute, P.O. Box 20345, MC 3-147, Houston, TX 77225-0345.

DOI: 10.1097/MAT.0b013e3181739b70

mathematical model, and the design and performance of the control system as a multivariable feedback unit.

Materials and Methods

Mock Circulatory System

The mock circulatory system we have designed is constructed of polyvinyl tubing (**Figure 1**), and comprises two CFPs (MicroMed Cardiovascular, Houston, Texas) in series, each with a compliance chamber and variable flow resistor, to represent the pulmonary and systemic portions of the circulatory system. Additional ventricular pressure simulators are omitted from the mock circuit to recreate the clinical scenario of a CFTAH system implantation, whereby both right and left ventricles are excised above the semilunar and atrioventricular valves, and each is replaced by a CFP. The inflow cannulae of the CFPs are removed; instead, flexible cuffs (latex membrane) are attached to the CFPs, allowing simulation of atrial collapse should venous return be inadequate. Systemic and pulmonary vascular resistances (SVR and PVR, respectively) were independently adjusted with variable flow resistors, which consisted of Harvard clamps placed on the outflow tubing of each pump. Although the flow in this mock circulatory system is nonpulsatile, the systemic and pulmonary vascular capacitances were important in damping pressure waves and decoupling pressures in the pulmonary and systemic circuits. The vascular capacitances were represented by the preset quantity of air in two sealed tanks (65 cm high, 12 cm diameter). Blood was represented by a solution of 35% glycerol in water at room

temperature, which had an approximate viscosity of 4 cP, and a total volume of approximately 5 liters.

We measured the aortic pressure (AoP), pulmonary artery pressure, left atrial pressure (LAP), right atrial pressure, systemic flow rate (Q_{sys}), and pulmonary flow rate (Q_{pul}) using the mock circulatory system. The sensor set comprised two tubing flow meters (Model P110, Transonic, Ithaca, NY) and four pressure transducers (Edwards LifeSciences, Irvine, CA). The pressure signals were conditioned using a low-pass, antialiasing filter, with a cut-off frequency of 25 Hz (Model 3364, Krohn-Hite, Brockton, MA). The data-acquisition system included a dSPACE control and data-acquisition board (dSPACE Inc., Novi, MI), and a computer equipped with MATLAB (Version 7.0.4, The MathWorks, Natick, MA) and ControlDesk (Version 2.6.5 Unicode, dSPACE GmbH, Germany). The dSPACE system also served as the real-time controller, which interfaced with the two pumps via an analog connection ("input voltage") to modified prototypes of the MicroMed clinical controllers. The chosen sampling frequency for this system was 100 Hz.

Using a dynamometer, we determined the relationship between pump speed and input voltage to each pump controller. The voltage range was approximately 3–6 V, corresponding to pump speeds of 6–14 krpm.

Mathematical Model

A set of algebraic and ordinary differential equations was developed to model the pressure and flow relationship of the various elements of the mock circulatory system and, therefore, the circulation (see Appendix B for details). Given that there are six elements to the mock circulatory system (**Figure 1**) and that each pump requires an additional equation for relating voltage to speed, eight equations are needed to model the circulation.¹² The inputs to the mock circulatory system (and the mathematical model) are the pump voltages, whereas the outputs are the pump flows in liter per minute. The mathematical model predicts perturbations in the systemic and pulmonary flows from their steady-state value. For instance, if systemic flow increases from 4 to 5 L/min, the output of the mathematical model for the systemic flow would be 1 L/min. The steady-state values of other parameters in the mock circulatory system and the mathematical model are shown in **Table 1**.

To validate the transient hemodynamic response of the mathematical model, we compared the two calculated flow rates with the measured flow rates of the mock circulatory system. In both the mathematical model and the mock circulatory system, we tested response to perturbation by rapidly

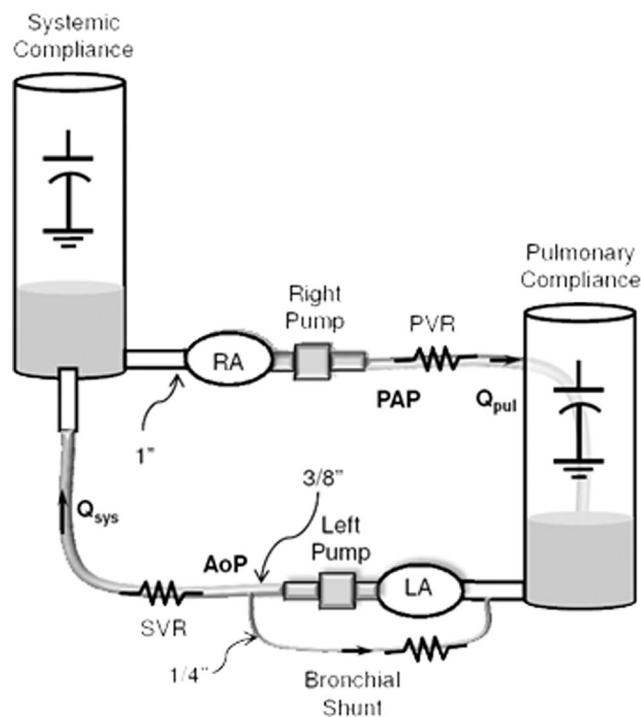


Figure 1. Schematic of the mock circulatory system. AoP, aortic pressure; LA, left atrium; PAP, pulmonary artery pressure; PVR, pulmonary vascular resistance; Q_{pul} , pulmonary artery flow rate; Q_{sys} , systemic flow rate; RA, right atrium; SVR, systemic vascular resistance.

Table 1. Steady-State Operating Conditions for the Mock Circulatory System and the Mathematical Model

Parameter	Steady-State Value
Q_{sys} , Q_{pul}	4.0–4.5 L/min
SVR	18 Wood units
PVR	2 Wood units
Left pump voltage	4.95 V
Right pump voltage	3.60 V

PVR, pulmonary vascular resistance; Q_{pul} , pulmonary flow rate; Q_{sys} , systemic flow rate; SVR, systemic vascular resistance.

oscillating pump speed for 10 seconds. This test was performed on the left pump, the right pump, and simultaneously on both pumps in separate experiments. Data were acquired for 30 seconds in the mock circulatory system and compared with values predicted by the mathematical model.

Feedback Control System

The feedback control system comprised a computerized controller for each pump of the CFAH. The controller received flow data and generated voltages based on a programmed algorithm that was derived from the mathematical model (see Appendix B). To illustrate the effectiveness of our flow control system, we simulated systemic and pulmonary hypertension states and recorded the flow response in the mock circulatory system both with and without the flow controllers under identical initial experimental conditions (pump speeds, SVR, PVR, etc.). Systemic hypertension was simulated by increasing SVR from 18 to 22 Wood units; pulmonary hypertension was simulated by increasing PVR from 2 to 10 Wood units. SVR and PVR were independently increased by turning the screw clamps on the mock aorta and pulmonary artery, respectively, 10 seconds after the start of data acquisition. Data were recorded for 100 seconds to demonstrate that the CFAH control system was stable over time.

The set-point for both Q_{sys} and Q_{pul} in the trials using flow controllers was 4.0 L/min; in the trials where flow control was not implemented in the mock circulatory system, the baseline Q_{sys} and Q_{pul} (before hypertension) equaled 4.0 L/min. Baseline left and right pump speeds were identical in the presence or absence of flow control for each respective simulated hypertension state. Data postprocessing was performed in MATLAB.

Results

The steady-state operating values of the variables in the mock circulatory system and the mathematical model are given in **Table 1**. The relationship between input voltage to each pump controller and pump speed was linear ($R^2 > 0.99$).

Mathematical Model

The response of Q_{sys} and Q_{pul} to simultaneous oscillation of left and right pump speeds is shown in **Figure 2**. This Figure compares the transient responses predicted from the mathematical model with the measured responses from the mock circulatory system. In **Figure 3**, the flow response to oscillation of right pump speed is shown. Note the perturbation in Q_{sys} despite the unchanged left pump speed, which is the result of autoregulation of left pump flow (Q_{sys}) in response to a change in left pump inflow pressure (LAP). **Figure 4** shows a comparable response with oscillation of left pump speed. **Figures 2–4** show a high degree of correlation between measured and computed Q_{sys} and Q_{pul} .

Experimental Validation of Feedback Controllers

Figure 5 shows the measured Q_{sys} and Q_{pul} once a systemic hypertension state (an increase in SVR from 18 to 22 Wood units) was initiated in the mock circulatory system. As shown

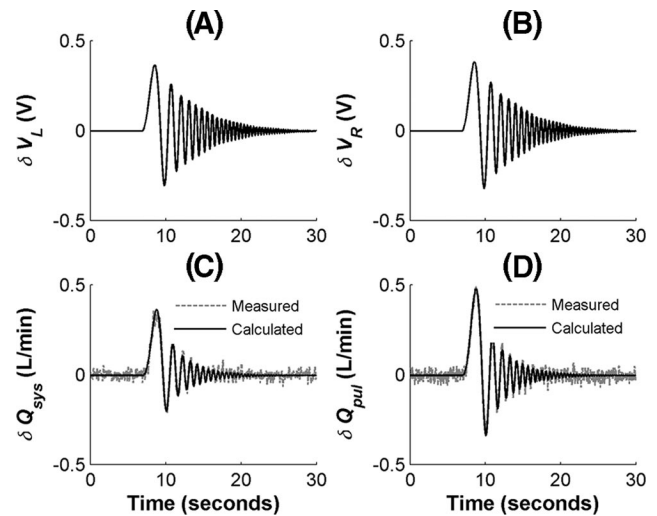


Figure 2. Comparison of the flow responses of the mock circulatory system and mathematical model due to swept sine wave input voltages to *both* pumps. The Figure shows perturbation in (A) left pump input voltage and (B) right pump input voltage and the measured and calculated changes in (C) systemic flow rate and (D) pulmonary flow rate. Q_{pul} , pulmonary flow rate; Q_{sys} , systemic flow rate; V_L , left pump input voltage; V_R , right pump input voltage.

in **Figures 5, A and B**, both Q_{sys} and Q_{pul} dropped by approximately 0.5 L/min in the absence of the flow controller. Left and right pump speeds remained at their baseline values of 11.01 and 4.82 krpm, respectively. In the presence of the flow controller, pump speeds were automatically adjusted by the controller to maintain constant flows. After systemic hypertension was simulated, Q_{sys} briefly decreased but returned to normal within 4 seconds (**Figure 5C**). Q_{pul} remained stable (**Figure 5D**). This flow response was achieved because the flow controller increased left pump speed to compensate for the reduced Q_{sys} while it maintained right pump speed close to its prehypertension value (**Table 2**).

Figure 6 shows the corresponding Q_{sys} and Q_{pul} measured in the mock circulatory system once pulmonary hypertension

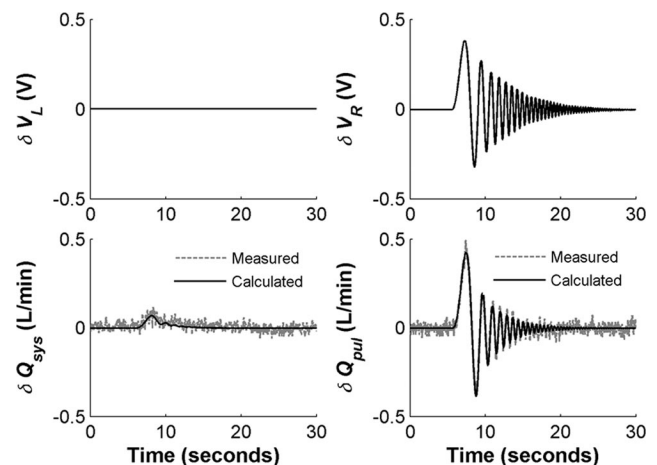


Figure 3. Comparison of the flow responses of the mock circulatory system and mathematical model due to swept sine wave voltages to the *right* pump only.

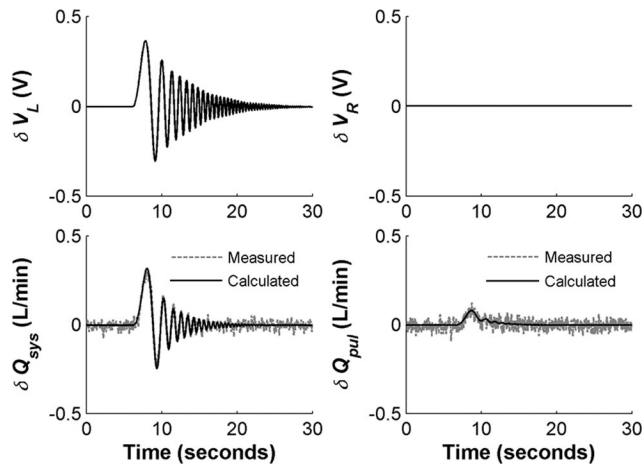


Figure 4. Comparison of the flow responses of the mock circulatory system and mathematical model due to swept sine wave voltages to the left pump only.

was simulated (an increase in PVR from 2 to 10 Wood units). In the absence of flow control (i.e., constant left and right pump speeds of 11.09 and 4.63 krpm, respectively), both Q_{sys} and Q_{pul} dropped by approximately 1 L/min, as shown in **Figures 6, A and B**. In addition, the decrease in fluid return to the left atrium (reduced pulmonary flow due to high PVR) caused collapse of the left atrial wall, which was confirmed by the characteristically abrupt decrease in Q_{sys} . In the presence of flow control, simulation of pulmonary hypertensive state resulted in a slight and temporary decrease in Q_{sys} and a decrease in Q_{pul} that lasted <4 seconds, but both flows returned to their baseline levels. The flow controller increased both left and right pump speeds to their final values shown in **Table 2** in order to maintain Q_{sys} and Q_{pul} at 4.0 L/min.

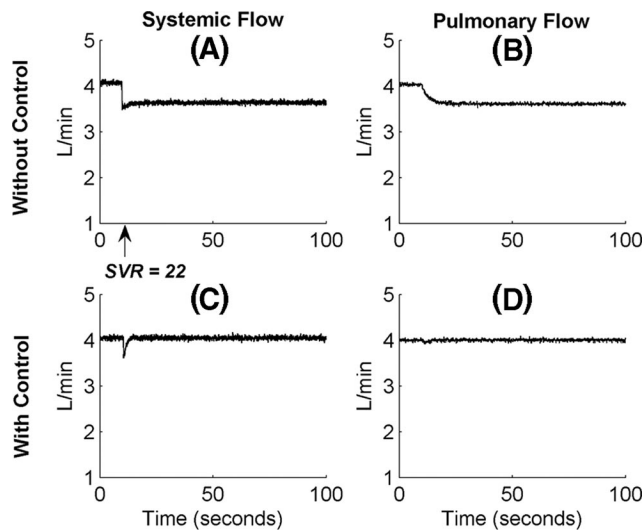


Figure 5. Simulation of systemic hypertension state due to increase in systemic vascular resistance (SVR) from 18 to 22 Wood units (arrow). Systemic and pulmonary flows are shown in the absence (A, B) and presence (C, D) of flow control.

Table 2. Mean Left and Right Pump Speeds (krpm) in the Presence of Flow Control Before and After Onset of Hypertension States in the Mock Circulatory System

	Left Pump	Right Pump
Systemic hypertension		
Baseline (SVR = 18)	11.01	4.82
Posthypertension (SVR = 22)	11.93	4.79
Pulmonary hypertension		
Baseline (PVR = 2)	11.09	4.63
Posthypertension (PVR = 10)	11.37	7.10

PVR, pulmonary vascular resistance (Wood units); SVR, systemic vascular resistance (Wood units).

Discussion

Although no clinical experience with the CFAH has been reported, previous work on the pulsatile TAH indicates the necessity for a control system to maintain balanced left and right pump flows.¹³ One of the advantages of the CFAH is the responsiveness of its flow output to both inflow pressure and outflow resistance and, therefore, its potential for flow auto-regulation.⁴ However, the need for a flow controller becomes inevitable if any perturbation to the circulatory system exceeds the autoregulatory capacity of either or both pumps of the CFAH. For example, the onset of pulmonary hypertension secondary to sudden pulmonary vasoconstriction (increase in PVR) or pulmonary edema would result in a sudden decrease in the right pump outflow, as shown in **Figure 6B**. Implementation of a flow controller promptly restores blood flow to a level compatible with normal physiology, as shown in **Figure 6D**.

In this study, Q_{sys} and Q_{pul} were chosen as the control variables because adequate and balanced left and right pump flows are of primary importance to achieve proper end-organ perfusion. The output variables were the voltages to the pump drivers, which regulated the rotational speed (rpm) of the two pumps independently. Thus, in both systemic and pulmonary

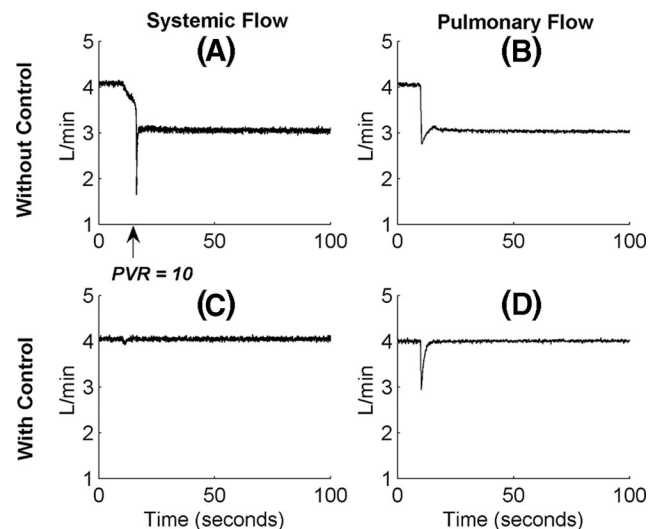


Figure 6. Simulation of pulmonary hypertension state due to increase in pulmonary vascular resistance (PVR) from 2 to 10 Wood units in the absence (A, B) and presence (C, D) of flow control.

hypertension states, the flow control system of the CFTAH simultaneously adjusted left and right pump speeds (**Table 2**) in order to maintain adequate and balanced flow in the systemic and pulmonary loops (**Figures 5** and **6**). Therefore, coordination of the two pump speeds relative to each other is also necessary if systemic and pulmonary flows are to accommodate a wide range of physiologic demands. Although the intrinsic automaticity of continuous flow pumps may make a sophisticated control algorithm superfluous, a control system may be valuable in the response to acute changes in vascular resistance such as may occur with exertion.

We have previously used aortic and pulmonary artery pressures as control variables with similar encouraging results.¹² Indeed, dual and multiple control variables may be regulated simultaneously by implementation of the so-called state-space control systems. Subsequent stages of our study will be geared to develop physiologic sensors, which will provide continuous, real-time data on control variables such as mixed venous oxygen saturation and pulmonary interstitial pressure, in addition to pump flows and pressures.

Our results suggest that the mock circulatory system may be of value in simulating the hemodynamics of an animal supported by dual pumps. Our mock circulatory system is similar to that developed by Donovan in that it includes a preload and afterload reservoir for each pump, which simulate the atrial and systemic/pulmonary compartments of the human cardiovascular system.¹⁴ However, in our design, we have included a bronchial return route from the aorta to the left atrium; *in vivo*, this shunt slightly increases the output of the left ventricle compared with the right, simulating an important (but often neglected) property of the natural circulation in mammals. For controller design and verification, this bronchial shunt was clamped to equate Q_{sys} and Q_{pul} but should be included if a more precise and realistic simulation is desired. In addition, the flexible atria allow us to simulate pump inflow collapse. The transparency of the mock system allows for visual assessment of fluid shift between the pulmonary and systemic portions of the mock circulation. The simplicity of its components makes this system easy to build and modify.

Limitations

Several assumptions and simplifications have been made in our *in vitro* and mathematical modeling of circulatory dynamics in the presence of a CFTAH. Our simulations of systemic and pulmonary hypertension were performed by rapidly increasing SVR and PVR, respectively, as this “step” input in vascular resistance is easy to produce in a mock circulatory system. Physiologically, changes in vascular resistance occur over a longer duration. The bronchial shunt has also been clamped for additional simplification. *In vivo* experiments are warranted for physiologic validation of the stability and robustness of the control system. In addition, further work is needed to test the effectiveness of the control system in correcting various pathophysiologic conditions, which are easier to simulate in the mock circulatory system than to induce in an experimental animal. Though our mock circulatory system has been valuable in the initial development and testing of the CFTAH feedback control system, it is a highly idealized model of the cardiovascular system. Additional refinements can be

implemented that will more closely mimic the physiology of the vascular system.

Conclusion

A novel mock circulatory system and mathematical model of the nonpulsatile circulation were used to design and test a physiologic flow controller for a CFTAH. The effectiveness of the flow control system was demonstrated by *in vitro* simulation of pulmonary and systemic hypertension states in the mock circulatory system. The control system was designed to work in conjunction with the autoregulating features of the CFTAH. In cases of either pulmonary or systemic hypertension, the control system responded to hemodynamic perturbations and maintained constant pulmonary and systemic flow rates. Further refinement of the control system may be warranted to address the potential need for flow adjustment during extremes of daily activity and other cardiovascular perturbations necessitating left and right pump speed coordination.

APPENDIX A

The flow rate of a continuous flow pump, under normal circumstances, depends on pump speed and the pressure differential (ΔP) across the pump. ΔP is simply the outflow pressure (afterload; determined by outflow resistance) minus the inflow pressure (preload). For the left pump of a CFTAH, the ΔP can be approximated by $\text{AoP} - \text{LAP}$. As LAP increases relative to AoP, the ΔP decreases resulting in an increase in pump flow. A decrease in AoP relative to LAP results in the same effect. This relationship between ΔP and flow rate can be graphically demonstrated on the pump characteristic curves. **Figure A1** shows the characteristic curve of an axial flow pump operating at 8 krpm. When the ΔP is high (point 1 in **Figure A1**, representing high AoP relative to LAP), the pump must overcome a greater load and therefore pumps less blood. If the outflow resistance, and therefore AoP, is reduced, the ΔP decreases and pump flow increases (point 2). These scenarios are also demonstrated in **Table 3**.

APPENDIX B

The linearized perturbation equations describing CFTAH and the mock circulatory system are shown below. Perturbation of each variable is denoted by δ . For example,

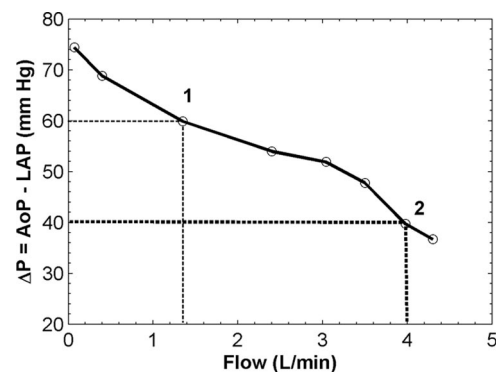


Figure A1. Pump characteristic curve of an axial flow pump at 8 krpm. ΔP , pressure gradient.

Table 3. Illustration of the Dependence of the Flow Rate of a Continuous Flow Pump on Pump Pressure Differential

AoP	LAP	ΔP	Flow Rate
— ↓	↑ —	↓ ↓	↑ ↑

AoP, aortic pressure; LAP, left atrial pressure; ΔP , pressure differential.

AoP = AoP⁰ + δ AoP, where AoP⁰ denotes the baseline value of AoP. The equations are

$$\delta Q_{\text{sys}} - \delta Q_{\text{pul}} = C_{\text{sys}} \delta R A P, \quad (\text{A1})$$

$$\delta Q_{\text{pul}} - \delta Q_{\text{sys}} = C_{\text{pul}} \delta L A P, \quad (\text{A2})$$

$$\delta A o P - \delta R A P = S V R \delta Q_{\text{sys}}, \quad (\text{A3})$$

$$\delta P A P - \delta L A P = P V R \delta Q_{\text{pul}}, \quad (\text{A4})$$

$$\delta A o P - \delta L A P = h_1 \delta \omega_L + h_2 \delta Q_{\text{sys}}, \quad (\text{A5})$$

$$\delta P A P - \delta R A P = h_3 \delta \omega_R + h_4 \delta Q_{\text{pul}}, \quad (\text{A6})$$

$$\tau_L \delta \dot{\omega}_L + \delta \omega_L = K_L \delta V_L, \quad (\text{A7})$$

$$\tau_R \delta \dot{\omega}_R + \delta \omega_R = K_R \delta V_R, \quad (\text{A8})$$

where a dot above a variable denotes its time derivative; C_{sys} and C_{pul} denote systemic and pulmonary capacitances, respectively; ω_L and ω_R are left and right pump speeds; V_L and V_R are left and right pump input voltages; and K_L and K_R as well as h_i (for $i = 1, 2, 3, 4$) are experimentally determined constants.

Conversion of the perturbation equations into transfer function form was performed using Mathematica 5.2 (Wolfram Research, Champaign, IL). The mathematical model relating flow rates (Q_{sys} and Q_{pul}) to input voltages (V_L and V_R) is given by

$$\begin{bmatrix} \delta Q_{\text{sys}} \\ \delta Q_{\text{pul}} \end{bmatrix} (s) = \begin{bmatrix} a_{11} & a_{12} \\ a_{21} & a_{22} \end{bmatrix} \begin{bmatrix} \delta V_L(s) \\ \delta V_R(s) \end{bmatrix}, \quad (\text{A9})$$

where

$$a_{11} = \frac{-h_1 K_L \left(s - \frac{C_{\text{sum}}}{C_{\text{eq}}(h_4 - P V R)} \right)}{\left(s + \frac{1}{\zeta} \right) \left(s + \frac{1}{\tau_L} \right)}, \quad (\text{A10})$$

$$a_{12} = \frac{h_3 K_R C_{\text{sum}}}{\left(s + \frac{1}{\zeta} \right) \left(s + \frac{1}{\tau_R} \right)}, \quad (\text{A11})$$

$$a_{21} = \frac{h_1 K_L C_{\text{sum}}}{\left(s + \frac{1}{\zeta} \right) \left(s + \frac{1}{\tau_L} \right)}, \quad (\text{A12})$$

$$a_{22} = \frac{-h_3 K_R \left(s - \frac{C_{\text{sum}}}{C_{\text{eq}}(h_2 - S V R)} \right)}{\left(s + \frac{1}{\zeta} \right) \left(s + \frac{1}{\tau_R} \right)}, \quad (\text{A13})$$

where s is the Laplace variable; h_i (for $i = 1, 2, 3, 4$) are as defined above; and

$$\zeta = \frac{C_{\text{eq}}(h_2 h_4 + R_{\text{eq}} - h_4 S V R - h_2 P V R)}{C_{\text{sum}}(R_{\text{sum}} - h_2 - h_4)}, \quad (\text{A14})$$

$$\begin{aligned} C_{\text{sum}} &= C_{\text{sys}} + C_{\text{pul}}, \\ R_{\text{sum}} &= S V R + P V R, \\ C_{\text{eq}} &= C_{\text{sys}} \cdot C_{\text{pul}}, \\ R_{\text{eq}} &= S V R \cdot P V R. \end{aligned}$$

The structure of the multivariable model of the CFTAH within the mock circulatory system is given in Eq. (A9). The diagonal terms of the multivariable model have one zero; the off-diagonal terms have no zeros; and the transfer function matrix is fully populated (*i.e.*, there is coupling between the systemic and pulmonary loops). Each element of the multivariable model has two poles. One pole (τ_L or τ_R) relates to the pump time constant and the other (ζ) to the fluid dynamics of the mock circulatory system. The coupling between the loops is a manifestation of the pumps' autoregulating properties—changes in inlet conditions result in changes in pump output. This coupling was considered during design of the controller.

To identify the model coefficients (K_L , K_R , and h_i), a multivariable system identification approach was used. A pseudo-random binary signal with a voltage input equivalent to 1 krpm amplitude served as the input signal to the left and right pumps of the mock circulation. The input signals were uncorrelated, and each was generated in Simulink (The MathWorks) by using the random number generator block with its output filtered via a 10th order low-pass Butterworth digital filter with cut-off frequency of 5 Hz (approximately 30 rad/s). This bandwidth ensured that the input signals were sufficient to excite the higher frequency dynamics of the system—namely, the dynamics of the pumps. The chosen sampling frequency in the mock circulatory system was 400 Hz. The antialiasing filters were low-pass Bessel filters with cut-off frequency of 100 Hz.

The multivariable parametric model was identified using the instrumental variables 4-step approach in MATLAB.¹⁵ The resulting parametric model was a discrete multivariable model that was mapped to the frequency domain (Bode plots). A continuous-time representation of the discrete system was then recovered from the Bode plots using the *invfreqs* command in MATLAB. The resulting parametric, continuous-time multivariable model of the CFTAH within the mock circulatory system is

$$\begin{bmatrix} \delta Q_{\text{sys}} \\ \delta Q_{\text{pul}} \end{bmatrix} (s) = \begin{bmatrix} 0.76 \frac{\left(\frac{s}{0.31} + 1 \right)}{\left(\frac{s}{0.42} + 1 \right) \left(\frac{s}{3.23} + 1 \right)} & 0.53 \frac{1}{\left(\frac{s}{0.42} + 1 \right) \left(\frac{s}{2.64} + 1 \right)} \\ 0.65 \frac{1}{\left(\frac{s}{0.42} + 1 \right) \left(\frac{s}{2.93} + 1 \right)} & 0.66 \frac{\left(\frac{s}{0.20} + 1 \right)}{\left(\frac{s}{0.42} + 1 \right) \left(\frac{s}{3.19} + 1 \right)} \end{bmatrix} \times \begin{bmatrix} \delta V_L(s) \\ \delta V_R(s) \end{bmatrix}, \quad (\text{A15})$$

where the outputs (perturbations in Q_{sys} and Q_{pul}) are measured in L/min and the inputs (perturbation in pump input voltages) are measured in V.

The proposed CFTAH controller is a *diagonal* multivariable controller where each diagonal term is an integral controller. This controller structure was chosen since integral controllers

cooperate with the autoregulation feature of the axial flow pumps, thus providing robust steady-state flow regulation without interfering with the inherent autoregulation of the CFTAH during transient conditions.

When designing a feedback controller, a precursor to closed-loop performance is closed-loop stability. For multivariable systems, closed-loop stability reduces to the guarantee of closed-loop stability for each diagonal closed-loop system provided the original multivariable system is diagonally dominant.¹⁶ The multivariable system (A15) is diagonally dominant, thereby reducing the multivariable controller design process to two single-loop designs.¹⁶ Although other multivariable controller design methodologies could be used, a single-loop classical controller design approach (loop shaping) is attractive when the controller structure is preconceived (in our case an integral controller) and when classical stability conditions (gain and/or phase margins) can capture the desired closed-loop performance. The single-loop controller design process employed is a frequency domain approach based on the so-called Nyquist Encirclement Condition.^{17,18} The Nyquist Encirclement Condition for open-loop stable systems reduces to simple amplitude and phase conditions imposed on the open-loop frequency response. To enforce closed-loop stability and performance, a phase margin constraint of at least 60° is imposed on each of the two open-loop transfer functions. This condition provides significant robustness of the CFTAH to changes in the vascular resistances and balances the closed-loop performance trade-offs between disturbance rejection and oscillations in the closed-loop system due to reference changes in the desired flow rates. Using the phase margin constraint for both loops, the designed multivariable controllers are

$$g_{11}(s) = g_{22}(s) = \frac{1.7}{s}. \quad (\text{A16})$$

Acknowledgments

We thank Mr. Scott Richardson (Levitronix LLC, Waltham, MA) and Mr. Mike Dingus (Mechanical Engineering, University of Houston) for their invaluable contributions to this work.

References

1. Frazier OH, Tuzun E, Cohn WE, *et al*: Total heart replacement using dual intracorporeal continuous-flow pumps in a chronic bovine model: a feasibility study. *ASAIO J* 52: 145–149, 2006.
2. Siegenthaler MP, Frazier OH, Beyersdorf F, *et al*: Mechanical reliability of the Jarvik 2000 Heart. *Ann Thorac Surg* 81: 1752–1758, 2006; discussion 1758–1759.
3. Saxton GA Jr, Andrews CB: An ideal heart pump with hydrodynamic characteristics analogous to the mammalian heart. *ASAIO Trans* 6: 288–291, 1960.
4. Khalil H, Cohn W, Benkowski R, *et al*: Preload sensitivity of continuous flow ventricular assist devices: application to the total artificial heart. *ASAIO J* 52: 41A, 2006.
5. Frazier OH, Tuzun E, Cohn W, *et al*: Total heart replacement with dual centrifugal ventricular assist devices. *ASAIO J* 51: 224–229, 2005.
6. Posch MG, Thompson LO, Koerner MM, *et al*: End-stage heart failure with multiple intracardiac thrombi: a rescue strategy. *Tex Heart Inst J* 31: 404–408, 2004.
7. Wu Y, Allaire PE, Tao G, Olsen D: Modeling, estimation, and control of human circulatory system with a left ventricular assist device. *IEEE Trans Control Syst Technol* 15: 754–767, 2007.
8. Giridharan GA, Pantalos GM, Gillars KJ, *et al*: Physiologic control of rotary blood pumps: an in vitro study. *ASAIO J* 50: 403–409, 2004.
9. Gwak KW, Ricci M, Snyder S, *et al*: In vitro evaluation of multiobjective hemodynamic control of a heart-assist pump. *ASAIO J* 51: 329–335, 2005.
10. Voigt O, Benkowski RJ, Morello GF: Suction detection for the MicroMed DeBakey Left Ventricular Assist Device. *ASAIO J* 51: 321–328, 2005.
11. Waters T, Allaire P, Tao G, *et al*: Motor feedback physiological control for a continuous flow ventricular assist device. *Artif Organs* 23: 480–486, 1999.
12. Khalil HA, Franchek MA, Kadipasaoglu KA, *et al*: Feedback control of the continuous flow total artificial heart. *ASAIO J* 52: 37A, 2006.
13. Abe Y, Chinzei T, Mabuchi K, *et al*: Physiological control of a total artificial heart: conductance- and arterial pressure-based control. *J Appl Physiol* 84: 868–876, 1998.
14. Donovan FM Jr: Design of a hydraulic analog of the circulatory system for evaluating artificial hearts. *Biomater Med Devices Artif Organs* 3: 439–449, 1975.
15. Ljung L: *System Identification, Theory for the User*. Upper Saddle River, NJ: Prentice Hall; 1999.
16. Rosenbrock HH: *Computer Aided Control System Design*. London: Academic Press; 1974.
17. Nyquist H: Regeneration theory. *Bell Syst Tech J* 1932;11.
18. Bode HW: *Network Analysis and Feedback Amplifier Design*. Princeton, NJ: Van Nostrand; 1945.